A MEMS gravimeter with multi-axis gravitational sensitivity

1st Richard P. Middlemiss
James Watt School of Engineering
University of Glasgow
Glasgow, UK.
richard.middlemiss@glasgow.ac.uk

2nd Paul Campsie
Biomedical Engineering Department
University of Strathclyde
Glasgow, UK.
paul.campsie@strath.ac.uk

3rd William Cunningham
Institute for Gravitational Research
University of Glasgow
Glasgow, UK.
william.cunningham@glasgow.ac.uk

4th Rebecca Douglas
Institute for Gravitational Research
rebecca.douglas@hindles.co.uk

5th Victoria McIvor
Institute for Gravitational Research
victoriamcivor@setventures.com

6th Vinod Belwanshi
Institute for Gravitational Research
vinod.belwanshi@glasgow.ac.uk

7th James Hough
Institute for Gravitational Research
james.hough@glasgow.ac.uk

8th Sheila Rowan
Institute for Gravitational Research
sheila.rowan@glasgow.ac.uk

9th Douglas J. Paul
James Watt School of Engineering
douglas.paul@glasgow.ac.uk

10th Abhinav Prasad
Institute for Gravitational Research
abhinav.prasad@glasgow.ac.uk

11th Giles D. Hammond
Institute for Gravitational Research
giles.hammond@glasgow.ac.uk

***Abstract*—A single-axis Microelectromechanical system gravimeter has recently been developed at the University of Glasgow. The sensitivity and stability of this device was demonstrated by measuring the Earth tides. The success of this device was enabled in part by its extremely low resonant frequency. This low frequency was achieved with a geometric anti-spring design, fabricated using well-established photolithography and dry etch techniques. Analytical models can be used to calculate the results of these non-linear oscillating systems, but the power of finite element analysis has not been fully utilised to explore the parameter space before now. In this article finite element models are used to investigate the behaviour of geometric anti-springs. These computer models provide the ability to investigate the effect of the fabrication material of the device: anisotropic <100> crystalline silicon. This is a parameter that is difficult to investigate analytically, but finite element modelling is used to take anisotropy into account. The finite element models are then used to demonstrate the design of a three-axis gravimeter enabling the gravity tensor to be measured - a significantly more powerful tool than the original single-axis device.**

***Index Terms*—MEMS, Gravimeter, Geophysics, Intertial Navigation**

I. Introduction

Gravimeters have applications in air and land-based oil and gas exploration [1], [2], sinkhole analysis [3], the detection of subterranean tunnels and cavities [4], CO_2 sequestration [5], geothermal reservoir monitoring [6], archaeology [7], hydrology [8], and volcanology [9]–[12]. Commercial gravimeters are all expensive ($100,000 USD) and use a range of different technologies for different applications. The commercially available gravimeters all require levelling, and this is carried out manually or be incorporating additional components to automate this process.

In previous work [14]–[16], the development of a low frequency microelectromechanical system (MEMS) gravimeter with a sensitivity of $4\times10^{-7}\,\mathrm{ms}^{-2}/\sqrt{\mathrm{Hz}}$ was discussed. This device has since been miniaturised and undergone field-testing [17]–[19]. A series of sensors are currently being built for integration within the NEWTON-g volcano gravity imager at Mt Etna, Sicily [20]. The device is capable of high acceleration sensitivity in part because of its extremely low resonant frequency MEMS resonator. This resonant frequency was achieved via the use of a geometric anti-spring design for the mass-on-spring system. A low resonant frequency means that the ratio is minimised between the spring constant, k, and the mass of the proof mass, m, giving a larger displacement for a given acceleration, and thus greater potential sensitivity for the gravimeter. An anti-spring can be characterised as having a negative or at least partially negative restoring force. As an anti-spring is extended, the spring constant decreases. One way to design an anti-spring is by using curved monolithic cantilevers, connected at a central point to constrain the motion vertically [21]. With the aim of achieving a high acceleration sensitivity for the MEMS gravimeter a monolithic geometric anti-spring configuration was chosen. A monolithic geometry

This work was funded by the Royal Society Paul Instrument Fund (STFC grant number ST/M000427/1), and the UK National Quantum Technology Hub in Quantum Enhanced Imaging (EP/M01326X/1). Dr R. P. Middlemiss is supported by the Royal Academy of Engineering under the Research Fellowship scheme (Project RF/201819/18/83).

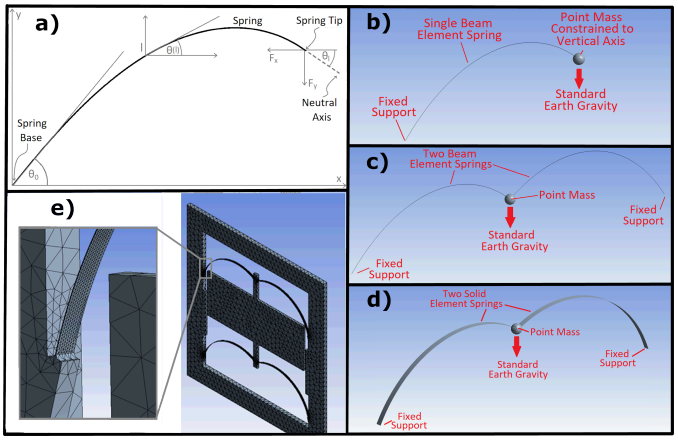

Fig. 1. The geometries of the springs used in the ANSYS finite element models. **a)** A simplified 1-dimensional analytical schematic diagram of the geometric anti-spring. **b)** The single spring model with boundary conditions applied to the free end to fix the displacement and rotation. A point mass of 8×10^{-6} kg is applied to the free end of the spring. This system is modelled using beam elements. **c)** The same model as **a)**, but with two symmetric springs and a point mass of 1.6×10^{-5} kg. In this model the boundary conditions on the free end are removed. **d)** The same design as 1c but with solid elements. In all cases a load step of 1 is equal to applying an acceleration of 9.8066 m/s^2. **e)** The final design of the 4-spring geometric anti-spring MEMS sensor, as modelled in ANSYS. The results of models conducted with this geometry would only converge if a dense mesh density was utilised over the springs.

was important because this allowed for the device to be fabricated from a single silicon chip.

II. Method and Results

A. Model Development

In order to verify the FE models of the MEMS based geometric anti-spring, a simple analytical model – based on the work of Cella et.al. [22] – was created. A schematic diagram of this model is displayed in figure 1a. The model outlines the parameters of a single geometric anti-spring blade. Such blades are never used individually; the proof mass is suspended from two or more symmetric blades, constraining it to move along a vertical axis; thus reducing the analytical problem to one dimension. The spring is clamped at the base with a launch angle of θ_0 and is constrained at the proof mass, or spring tip, by an angle θ_L. This results in a boundary value problem that can be conveniently solved in MATLAB with the *bvp4c* algorithm [24].

As mentioned above, the tip of the geometric anti-spring is constrained to move along a vertical line. This is equivalent to requiring that the horizontal position of the tip always maintains a constant value. This constraint is defined via the compression ratio $x_{\text{com}} = x_{\text{tip}}/L$. As the vertical displacement and/or compression ratio increases, the 2$^{\text{nd}}$ spring provides the force G_x, which introduces the negative component of the spring constant (the 2$^{\text{nd}}$ spring is not displayed in figure 1a, but it is symmetrically mirrored in the vertical plane that intersects the spring tip). This is the reason why the term "geometric anti-spring" is used; the anti-spring nature comes from geometry alone.

To assess characteristics of the spring that could not be investigated using the analytical model, a series of simple spring systems were built using ANSYS workbench v17 software. The geometric parameters (launch angle etc.) of the springs in each model were identical to those presented in figure 1a. Three initial FE simulations were performed to verify that the ANSYS model could correctly determine the displacement-force curves of the geometric anti-spring system. First a single spring with a point-mass was tested (see figure 1B), and then a more realistic two-spring system. This system was built using both beam elements (figure 1c) and solid elements (figure 1d). Excellent agreement was observed between the analytical and FE models. This confirmation meant that the simple analytical model could be utilised to test and optimise new geometries. Conversely, the full FE model would be useful for determining the effect of varying spring geometries caused by non-ideal etching tolerances; in addition to exploring the stress in the springs and the effect of crystalline silicon. Since silicon is a crystalline material and thus exhibits a Young's modulus that depends on the orientation of the crystal axis to the etched device. It is particularly important to utilise the correct Young's modulus in FE simulations in order to accurately predict the ultimate displacement/resonant frequency of the MEMS device since the moduli can vary by up to 45% [25] depending on the axis. The modulus tensor provided by Hopcroft et. al. [25] was utilised.

For gravimetry applications there is a desire to develop low frequency resonators that provide stable behaviour. It would therefore be beneficial to have a simple means of tuning the resonant frequency for a fixed proof mass. This is generally achieved by reducing the compression ratio of the spring system $x_{\text{com}} = x_{\text{tip}}/L$. For MEMS systems, however, in which the springs are etched, there is no capability to actually change the horizontal compression ratio as this is just set by the initial geometry of the MEMS mask. As mentioned earlier, a convenient way to alter the frequency is to change the launch angle of the spring. This has the effect of increasing the arc length of the spring, L, which in-turn reduces the compression ratio for a given x_{tip}. It was observed that as the launch angle increases the resonant frequencies drops (see figure 2). An additional means of tuning the system is to alter the ratio of k/m. It was found that by altering the spring thickness, the level of loading at which the oscillator reaches its minimum frequency can be changed (see figure 3). It was also observed that changing the thickness of the spring (whilst keeping the mass constant) does not change the minimum frequency of the system substantially (compared to the change that can be induced by altering the launch angle). The following protocol could therefore be followed in order to tune the design of a MEMS geometric anti-spring. First, the launch angle could be chosen to determine the minimum frequency. With this launch angle fixed, the thickness of the springs could then be altered in order to set the loading at which this minimum frequency is achieved. For situations in which changes in vertical gravity

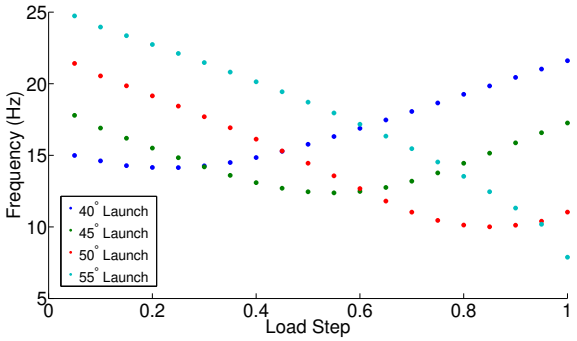

Fig. 2. Launch Angle Comparison. The greater the launch angle, the lower the resonant frequency.

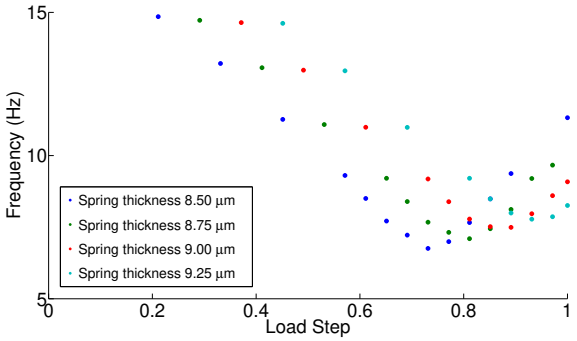

Fig. 3. Spring Thickness Comparison. The level of loading at which the frequency minimum occurs can be tuned by altering the thickness of the spring.

need to be measured, it would be necessary for the frequency minimum to occur at full loading (i.e. suspended vertically in the Earth's gravitational field). It is not always the case that gravimeters would be operated in such a vertical configuration, as will be discussed in Triaxial MEMS Gravimeter section.

The next stage of the investigation was to model a full MEMS gravimeter. Such a device requires four springs to support a central mass (see figure 1e). With only two springs the system would only be stable when vertical: if rotated sideways torsional stresses would break the springs. Four springs are utilised so that the system is self-supporting in any orientation.

In this model a minimum element size of 4.25×10^{-6} m was utilised. This system has a minimum resonant frequency when vertical of around 5 Hz and a maximum equivalent stress in the spring of 200 MPa. From our previous studies, and measurements of the breaking stress in in thin silicon suspension beams [26] this seems an appropriate level of stress to provide a robust device. A very dense mesh is required across the springs of the model, especially where the springs meet the frame and the proof mass. This is where most of the motion and therefore most of the stress is concentrated. Tests were carried out on the mesh density to confirm that the model converges. This model was then used to consider the design characteristics of a tri-axial gravity sensor.

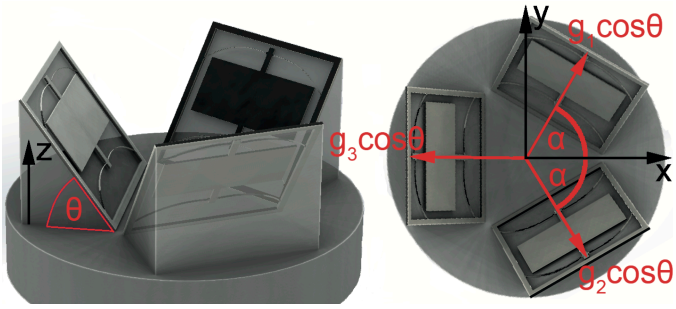

Fig. 4. A Future Gravimeter Design. A computer generated image of a three-axis MEMS gravimeter in a Galperin configuration [23].

B. The Design of Future Triaxial MEMS Gravimeters

After the behaviour of the anisotropic silicon anti-spring was understood, more complex designs of gravimeters could be considered. All previous works on this topic by the authors have concentrated on gravimeters that operate in a vertical configuration. These cannot be used to measure variations in acceleration other than those in the vertical, z, component of gravity. It is possible, however, to design a gravimeter that has sensitivity to the x, y, and z components of gravity, not just z. Such a gravimeter has the advantage that providing the orientation of the device is known, the levelling requirements are not as stringent as those for a one dimensional gravimeter measuring only the z-component. Making such a device is only possible if the angle at which the minimum frequency (where the optimum acceleration sensitivity occurs) is tunable. As already discussed it is possible to tune both the minimum frequency, and the loading at which this frequency occurs. Since the angle of the device is just a proxy for loading (along with spring thickness, and the mass value), one could easily design a device that would reach its minimum frequency at a specific angle. In such a device three tuned MEMS devices could be placed in the Galperin configuration [23] at an angle of $\theta = 54.7°$ from the horizontal, and separated azimuthally from each other at an angle of 120° (see Fig. 4). The Galperin configuration was designed to allow three identical sensors to measure gravity (or seismic activity) in three dimensions. Conversely, if one wanted to mount three sensors parallel to x, y and z, then two different sensor geometries would be required. This is because the sensors in x and y would be perpendicular to the 1 g field, and the sensor in z would be parallel to it. The devices in x and y would consequently experience different forces to the device in z.

For a triaxial device such as that presented in figure 4, the acceleration in each of the three axes would be given by equations 1, 2 and 3:

$$g_z = \frac{(g_1 + g_2 + g_3)\sin\theta}{3} \tag{1}$$

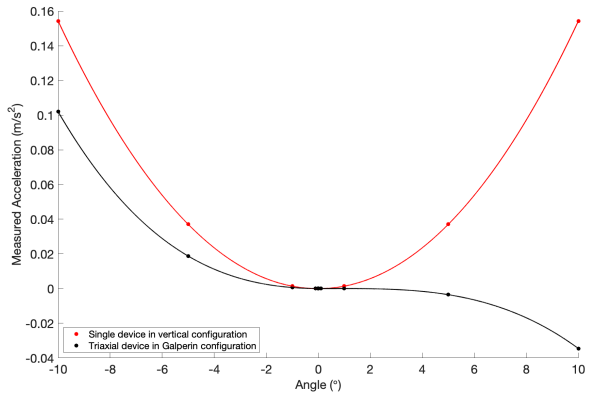

Fig. 5. Tilt Susceptibility Comparison. A comparison between the tilt susceptibility of a single vertical sensor, and that of three devices placed in a triaxial configuration.

$$g_x = ((g_1 + g_2)\cos\alpha)\cos\theta - g_3\cos\theta \tag{2}$$

$$g_y = ((g_1 - g_2)\sin\alpha)\cos\theta \tag{3}$$

To test the susceptibility of such a triaxial model to tilt, a geometry was tuned so that its minimum frequency would occur at the Galperin angle. Three identical models of this kind were then set up to match the configuration detailed in figure 4. The acceleration vectors of these models were then varied to simulate the effect of a tilting base plate. The displacement and resonant frequencies of each of the proof masses were measured, and a value of gravitational acceleration calculated using $g_i = \omega^2 x$ (where g_i is the output of one of the individual sensors). The total parasitic acceleration in g_z (see eq. 1) due to tilt was then plotted to ascertain whether tilt susceptibility was better in this configuration than for a single MEMS chip oriented vertically in a gravitational field. Figure 5 shows the results of this test. It can be seen that the triaxial configuration is less sensitive to tilt than a single vertical sensor.

III. Conclusion

Since the triaxial system offers multi-axis sensitivity, as well as a reduced tilt susceptibility, it is clear that this design would provide practical benefits in the many industries that utilise microgravity surveys. Crucially, however, tensor measurement of the gravitational field is an essential characteristic of an inertial navigation device. The use of MEMS devices for inertial navigation has become a possibility in recent years [13]. Any MEMS device, however, will suffer from drift – so long-term navigation would be susceptible to errors that increase with time. Whilst MEMS devices have been utilised for inertial navigation, to the knowledge of the authors, no MEMS device has yet been developed that has both triaxial sensitivity *and* the temporal stability of the sensors developed by the authors [14].

References

[1] G Barnes, and J. Barraud, "Imaging geologic surfaces by inverting gravity gradient data with depth horizons," Geophysics, vol 77, pp. G1–G11, 2012

[2] H. Rim, "Advantages of borehole vector gravity in density imaging," Geophysics, vol 80, pp. G1–G13, 2015

[3] G. Kaufmann, "Geophysical mapping of solution and collapse sinkholes," Journal of Applied Geophysics, vol. 111, pp. 271–288, 2014

[4] A. Romaides *et al.*, "A comparison of gravimetric techniques for measuring subsurface void signals," Journal of Physics D: Applied Physics, vol. 34, pp. 433–443, 2001.

[5] E. Gasperikova, E., and G. M. Hoversten, G. M., "Gravity monitoring of CO2 movement during sequestration: Model studies," Geophysics, vol. 73, pp. 1ND–Z105, 2008.

[6] J. Nishijima, *et al.*, "Repeat Absolute and Relative Gravity Measurements for Geothermal Reservoir Monitoring in the Ogiri Geothermal Field, Southern Kyushu, Japan," IOP Conference Series: Earth and Environmental Science, vol. 42, pp. 012004, 2016

[7] J. Panisova, R. Pasteka, "The use of microgravity technique in archaeology: A case study from the St. Nicolas Church in Pukanec, Slovakia," Contributions to Geophysics and Geodesy, vol. 39, pp. 237–254, 2009

[8] B. Fores,C. Champollion, N. Le Moigne, R. Bayer, and J. Chéry, "Assessing the precision of the iGrav superconducting gravimeter for hydrological models and karstic hydrological process identification," Geophysical Journal International, vol. 208, pp. 269–280, 2017.

[9] J. Fernández, A. Pepe, M. P. Poland, and F. Sigmundsson, "Volcano Geodesy: Recent developments and future challenges," Journal of Volcanology and Geothermal Research, vol. 344, pp. 1–12, 2017

[10] D. Carbone, M. P. Poland, M. Diament, and F. Greco, "The added value of time-variable microgravimetry to the understanding of how volcanoes work", Earth-Sci. Rev., vol. 169, pp.146–179, 2017

[11] M. Battaglia, J. Gottsmann, D. Carbone, and J. Fernandez, "4D volcano gravimetry," Geophysics, vol. 73, pp. WA3–WA18, 2008.

[12] H. Rymer, G. Williams-jones, and M Keynes, "Gravity and Deformation Measurements," Geophysical Research Letters, vol. 27, pp. 2389–2392, 2000

[13] O. J. Woodman, "An introduction to inertial navigation. No. UCAM-CL-TR-696," University of Cambridge, Computer Laboratory, 2007.

[14] R. P. Middlemiss, *et al.*, "Measurement of the Earth Tides with a MEMS Gravimeter," Nature, vol. 531, pp. 614–617, 2016

[15] P. Campsie, G. Hammond, R. P. Middlemiss, D. J. Paul, and A. Samarelli, "Measurement of Acceleration, US Patent Number: 10802042, 2015

[16] R. P. Middlemiss, "A Practical MEMS Gravimeter," PhD Thesis, University of Glasgow, 2016

[17] R. P. Middlemiss *et al.*, "Field Tests of a Portable MEMS Gravimeter," Sensors, vol. 17, pp. 2571, 2017

[18] S. G. Bramsiepe, D. Loomes, R. P. Middlemiss, D. J. Paul, and G. D. Hammond, "A High Stability Optical Shadow Sensor with Applications for Precision Accelerometers," IEEE Sensors Journal, vol. 18, pp. 4108–4116, 2018

[19] R. P. Middlemiss *et al.*. "Microelectromechanical system gravimeters as a new tool for gravity imaging," Phil. Trans. R. Soc. A, vol. 376, 2018.

[20] D. Carbone *et al.*, "The NEWTON-g Gravity Imager: Toward New Paradigms for Terrain Gravimetry," Frontiers in Earth Science, vol. 8, 2020

[21] R. Ibrahim, "Recent advances in nonlinear passive vibration isolators," J.Sound Vib., vol. 314, pp. 371–452, 2008

[22] G. Cella, V. Sannibale, R. Desalvo, S. Márka, and A. Takamori, "Monolithic geometric anti-spring blades," Nucl. Instr. Meth. Phys. Res. A, vol. 540, pp. 502–519, 2005

[23] E. Galperin, "Azimuthal method of seismic observations," Gostoptechizdat, Moscow, vol. 80, 1955

[24] L. F. Shampine, and M. W. Reichelt, "Solving Boundary Value Problems for Ordinary Differential Equations in Matlab with bvp4c," MATLAB Technical Report, pp. 1–27, 2000

[25] M. Hopcroft, W. Nix, and T. Kenny, "What is the Young's modulus of silicon?," J. Microelectromech. Syst., vol. 19, pp. 229–238, 2010

[26] A. Cumming *et al.*, "Silicon mirror suspensions for gravitational wave detectors," Class. Quantum Grav., vol. 31, pp. 025017, 2014